ISSN: 2689-1204

Research Article

Journal of Applied Material Science & Engineering Research

Efficient removal of organic pollutants in wastewater using tin oxide nanospheres under photoirradiation

Mandeep Kaur[1], Mamta Belwal[2], Aakriti Sharma[3], Ashish Kumar[4*] and Venkataraman Vishwanathan[5]

[1]*Department of Biophysics, Panjab University, Chandigarh-160014, India*

[2]*Departnment of Chemistry, Radhey Hari Government Post Graduate College, Kahipur-244713, Uttarakhand, India.*

[3]*Department of Chemical Engineering, Indian Institute of Technology Ropar-140001, Punjab, India*

[4]*Depatment of Chemistry, Hemawati Nandan Bahuguna Government Post Graduate College, Khatima - 262308, Uttarakhand, India.*

[5]*Applied Sciences Department, Faculty of Engineering and Applied Sciences, Botho University, Gaborone, Botswana*

[*]Corresponding author
Ashish Kumar, Depatment of Chemistry, Hemawati Nandan Bahuguna Government Post Graduate College, Khatima – 261308, Uttrakhand, India

Submitted: 14 July 2020; **Accepted**: 20 July 2020; **Published**: 30 Dec 2020

Abstract

The maximum toxic pollutants discharged by the industrial and domestic wastewater effluents are the pathogens and organic chemicals. Recently, mesoporous tin oxide (SnO2) nanospheres have gained attention as a suitable material in photodegrdation of poisonous pollutants like methylene blue (MB) and chlorobenzene (CB) when exposed to Ultraviolet and Visible irradiation. In this study, a single step synthesis of SnO2 nanospheres with large surface area (104 m2g−1) was prepared from mixing two different types of surfactants. Pertinent physico-chemical characterisation techniques such as X-ray diffraction (XRD), scanning electron microscopy (SEM), high resolution transmission electron microscopy (HRTEM), energy dispersive X-ray spectroscopy (EDS), and N2 adsorption–desorption measurements were used to get an insight into the structural details of the freshly prepared SnO2 nanospheres. Results showed that SnO2 samples were spherical in shape and with an average size of 2-5 nm. According to the pseudo 1st order kinetic study, a rate constant (k) of 0.02693 min−1 and 0.02136 min−1 for methylene blue (MB) and 0.2385 and 0.2023 for chlorobenzene (CB) were observed under UV and visible irradiation, respectively. High photoactivity of SnO2 nanospheres may be ascribed to its reduced crystalline size and high surface area. Also, the SnO2 nanospheres showed high response, selectivity, and good recovery rate towards degradation.

Keywords: Tin Oxide, Nanoparticles, Chlorobenzene, Visible Irradiation, And Methylene Blue

Introduction

Recently, the combination of porous structures and nanomaterials have become the most fascinating areas of research. These materials can be of different shapes and sizes with the mesoporous range usually falling between 2 and 50 nm. They have been given more importance due to their myriad application in the industrial sectors [1]. Among the different kinds of porous materials, mesoporous SnO2 plays an important role. There are various preparatory methods are known while preparing SnO2 like. solvent-free infiltration, microemulsion, sol-gel hydrolysis, solvothermal, hydrothermal and so on. Most of the preparatory routes lead to agglomeration of smaller particles into larger crystallite size [2-6]. To make smaller crystallites of SnO2 nanospheres, they are prepared from mixing suitable surfactants [7].

Surfactants gives the desired pore size to the nanoparticles due to the type of bonding it creates between counter ions. The long alkyl chains of surfactants help in forming many smaller pores in SnO2

nanospheres at the time of synthesis [8]. Various types and combination of surfactants have shown different morphologies and pore sizes. In our present investigation an attempt has been made to synthesis mesoporous SnO2 nanospheres using a mixture of cationic and anionic surfactants with specific molar ratios to give a high surface area material.

Photoadsorption of toxic materials from wastewater on semiconducting oxide surfaces is economical and non-toxic in removal of organic dyes [9]. Photo-oxidation is gaining interest because of its efficiency in the degrading toxic pollutants arising from the waste pesticides, petroleum refining, detergents, textile processing, fertilizers etc. Degradation of these harmful pollutants is quite difficult and complex. They create many serious ecological problems, owing to environmental pollution. Photocatalysis is an efficient method to clean up the polluted water. Methylene blue and chlorobenzene, are water-soluble dyes, used by textile manufacturers have a serious carcinogenic effect and release aromatic amines. These synthetic dyes are non-degradable by nature and create threat to aquatic life as well. Many conventional methods such as filtration, sedimentation and adsorption on activated carbon etc. are employed to minimize the hazardous effect of wastewater containing dye.

The objective this study was to synthesis mesoporous SnO_2 nanospheres by the solvent-free single step method using a mixture of two surfactants (namely, cationic and anionic) and to test them as a photocatalyst to decompose the two pollutants (MB and CB) under UV and Visible light. SnO_2 is basically a n-type semiconductor having a Eg value of 3.6 eV. The SnO_2 samples were characterized for their structural and textural properties using conventional physical, chemical and spectroscopic techniques.

Materials and Methods

Preparation of Mesoporous Sno_2 Nanospheres

Tin (II) chloride or stannous chloride ($SnCl_2.H_2O$) precursor was used as a source for the synthesis of mesoporous tin oxide (m-SnO_2). CTAB and SDS were used as cationic and anionic surfactants, respectively to enhance the specific surface area of SnO_2 nanospheres. A solution of $SnCl_2.H_2O$ (1.0 M) was added to the mixture of SDS (0.25 M) + CTAB (0.25 M) and stirred for an hour. Freshly prepared 1.0 molar NaOH was added to the reactant mixture so as to precipitate $Sn(OH)_2$. The solid mass was washed with ¬¬¬distilled water, dried and calcined at 600 °C for 4 hours.

Mechanism of Formation of M-Sno_2 Nanospheres

Appropriate molar quantities of the two surfactants, CTAB and SDS when mixed together, they form spherical micelles. The weak interaction between the surfactants give rise to the formation of a well organised spherical micelles [10]. Mixtures of surfactants show more activity than individual ones in producing nanospheres. The two groups, sulphate and bromide from the surfactants bind the stannous ions in forming the zwitterions structures [11]. Figure 1 describes the formation of mesoporous SnO2 nanospheres.

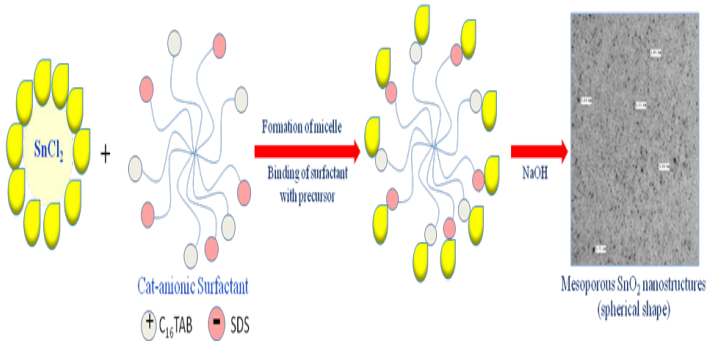

Figure 1: Mechanism showing the formation of spherical SnO2 nanospheres.

Characterisation

The physico-chemical properties of mesoporous SnO_2 were investigated using X-ray powder diffraction (XRD) technique to determine the crystalline phase of SnO_2 sample. The surface morphology of the samples was studied with electron microscopy (scanning as well as transmission). While, Energy-dispersive spectroscopy (EDS) was used to find the elemental compositions of SnO_2 nanospheres. Nitrogen adsorption-desorption measurements were made at 77K to calculate the surface area and pore distribution (size and volume) of the nanospheres, using BET and BJH methods, respectively.

Photoactivity Study

The synthesised mesoporous SnO_2 nanospheres were tested for the degradation of MB and CB present in the wastewater sample. About 20 mg of SnO_2 was added in a 10 mL water solution of MB or CB. It was then irradiated with a mercury lamp or CFL lamp for 120 min. The sample solution and the lamp were kept apart by 10 cm. The entire system was kept in a closed vessel under ice bath to maintain a constant temperature. After the completion of photoirradiation, the SnO_2 was separated from the sample solution and the spectra was run using UV–Visible spectrophotometer. The absorbance spectra were recorded at a known time interval at 665 nm and 263 nm, respectively. Using Beer Lambert's law, i.e. concentration of the sample solution is proportional to absorbance, the percentage of photo efficiency was measured as shown in Eqn.1:

$$\text{Rate} = \{(C_0 - C) / C_0\} \text{ X } 100 = \{(A_0 - A) / A_0\} \text{ X } 100 \qquad (1)$$

where C_0, C and A_0, A, are the solution concentration and absorbance values of the sample solution at initial and final stages at time t = 0 and t, respectively. The kinetic rate constant (k) was calculated from the pseudo 1st order reaction as:

$$\ln C/C_0 = -kt \qquad (2)$$

where C0 and C are the concentration of the solution at the initial and final stages of the reaction.

Results and Discussion

X-ray Powder Diffraction (XRD) Analysis

The XRD profiles of freshly calcined mesoporous SnO_2 nanospheres are shown in Figure 2. The sample, SnO_2 exhibited several diffraction peaks at 2θ of 26.77°, 34.14°, 38.12°, 51.93°, 54.97°, 58.20°, 62.16°, 64.98°, 66.25°, 71.49° and 78.98°, which corresponded to tetragonal rutile structure of SnO_2 [12]. It is interesting to observe the absence of other peaks except 'Sn' and 'O', suggesting the presence of only pure tin oxide (SnO_2). The average crystallite size of SnO2 was 5.05 nm, as calculated from Debye-Scherrer equation using the diffraction peak of (1 1 0) [13].

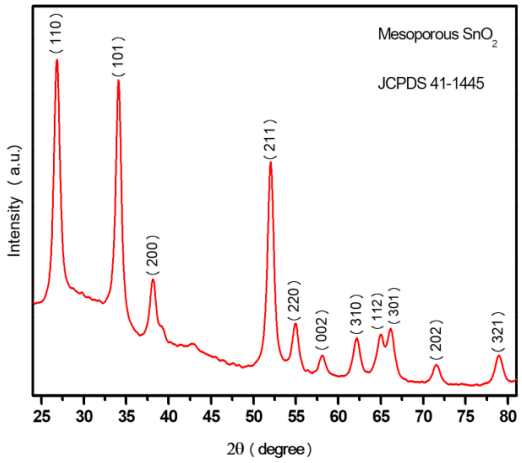

Figure 2: XRD patterns of SnO_2 nanospheres

Morphological Analysis

The spherical morphology of SnO_2 was ascertained from TEM analysis. **Figure 3(a)** shows the high resolution TEM images of freshly prepared SnO_2. They are of spherical shape with size ranging from 2 to 5 nm. The mesoporous structures of SnO_2 was further investigated using scanning electron microscopy as shown in **Figure 3(b)**. It confirms further the spherical structures of SnO_2. The elemental distribution of SnO_2 was established by the EDS analysis **(Figure 3c)**. The existence of Sn and O atoms only in the prepared SnO_2 sample in the EDS spectra suggest the absence of any elemental impurities appears during the synthesis of SnO_2 nanospheres.

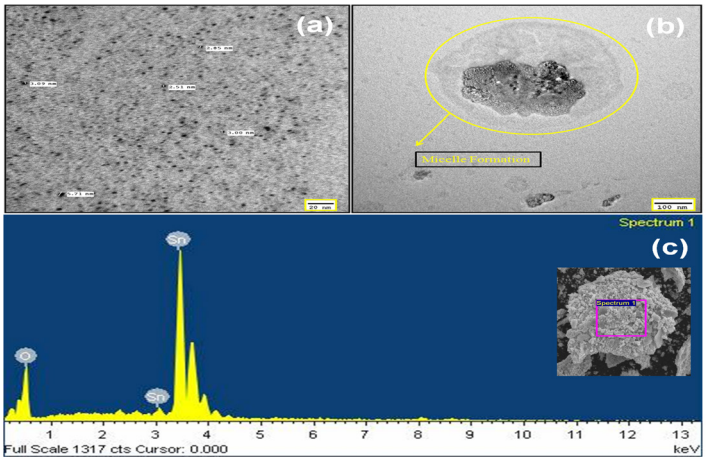

Figure 3:(a) High resolution TEM image, (b) Field emission SEM image and (c) EDS spectrum of SnO_2 nanospheres.

N2 Adsorption/Desorption Analysis

The surfactant when adsorbed on the surface of the nanospheres, it significantly reduced the formation of large crystallites of SnO_2 [14]. **Figure 4 (a)** shows the N2 adsorption–desorption curves of the freshly calcined SnO_2. Type IV isotherm was observed with a hysteresis loop and shows an increase of P/Po between 0.4 and 0.9. The BET area of SnO2 nanospheres, using the mixture of surfactants was found to be 104 m^2g^{-1}. The mixture of cationic and anionic surfactants yielded a high surface area as compared to the individual surfactant (surface area of CTMB = 8.45 and SDS = 7.23.m^2g^{-1}). This may be due to the electrostatic attraction between metal ions (positive charge) and SDS (negative charge), a sizeable micelle formation may take place. The differential BJH plot of SnO_2 nanospheres is shown in **Figure 4(b)**. The pore volume and mean diameter were observed to be 0.140 cm^3g^{-1} and 5.37 nm, respectively.

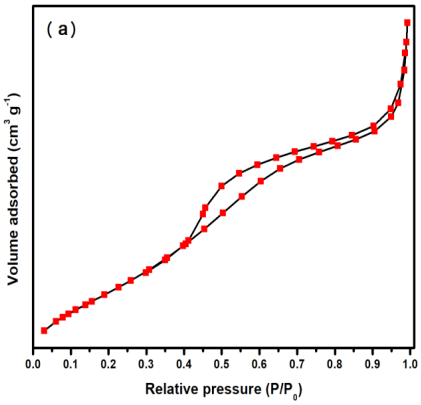

Figure 4: (a) N_2 adsorption-desorption isotherm; and (b) BJH pore size distribution of SnO_2 nanospheres.

Photocatalytic Degradation of MB and CB

In a blank run, we observed that SnO_2 did not decompose either MB or CB in the dark. However, in the absence of SnO_2, when the sample solution was irradiated, it showed a degradation of 5 to 8% within 1 hour of incubation. This suggests that both the light source as well as the presence of SnO_2 nanospheres should be necessary for the reaction. It suggests that the SnO_2 nanospheres have the good capacity to absorb the light and to mineralise the pollutants present in the solution.

In a typical run, the decomposition of the sample solution containing MB or CB was monitored in the absorption peak corresponding to 665 nm in the UV-Visible region. **Figure 5a** shows the spectra of the MB along with SnO_2 present in the solution at different time interval. The photo activity was found to be higher due to its high surface area and pore volume of SnO_2 nanospheres. The maximum degradation efficiency of MB was found to be 80% within 60 min.

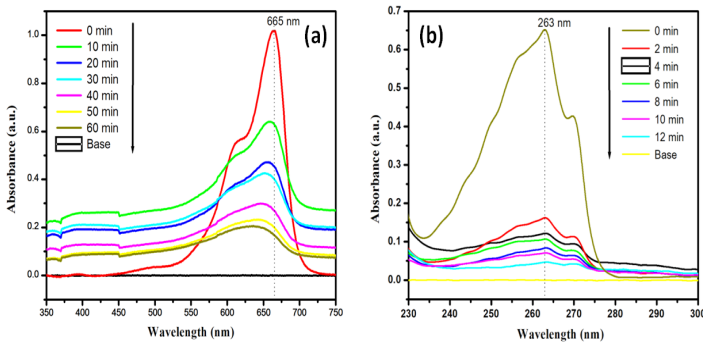

Figure 5: Time dependent UV–Visible absorption spectra of the photocatalytic degradation of (a) methylene blue and (b) chlorobenzene in presence of SnO_2 nanospheres

This suggests that the photo activity of the resulted material is a function of the interface between SnO2 and the pollutant. Larger specific surface area of the adsorptive material may be desired to be in contact with organic molecules. In a similar way, the photodecomposition of CB was carried out after achieving adsorption-desorption equilibrium in dark within 60 minutes. Under UV light, rapid degradation was observed (Figure 5b). The sample solution of CB showed the best photoactivity of 93% within 12 min

According to the kinetic study, the photodecomposition over SnO_2 nanosphere follows a pseudo 1st order kinetics. The corresponding reaction constant (k) was determined from Eqn. 2 and are reported in Table 1.

Table 1: Rate constant (k) values for MB and CB over SnO2 nanospheres.

Photocatalyst	*k* values for MB / (min^{-1})		*k* values for CB / (min^{-1})	
	UV source	Visible source	UV Source	Visible source
SnO_2	0.02693	0.02136	0.2385	0.2023

According to Eqn.2, the plot of $\ln(C/C_0)$ against time should be linear. **Figure 6 (a & b)** confirmed that both MB and CB decomposed as a pseudo 1st order reaction. From the data

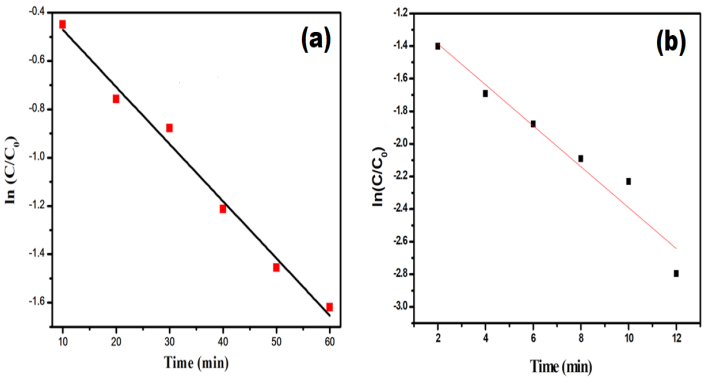

Figure 6: Kinetic analysis of (a) methylene blue and (b) chlorobenzene, in presence of SnO2 nanospheres.

Shown, one could infer that SnO_2 has a higher k values for MB than CB during mineralisation under UV-Visible irradiation.

Mechanism of Photodegradation

Based on the above discussion, the photo mechanism for the mineralization of MB or CS may be described as follows: Irradiation of SnO_2 surface with enough energy, dissociates the exciton (h^+-e^-) separately into holes (h^+) and electrons (e^-). The holes (h^+) remain in the valence band (VB) while the electrons (e^-) move to the conduction band (CB). The hole oxidises oxidizes either the pollutant directly or the water into hydroxyl (OH*) radical. At the same time, the electron presents in the CB. reduces the oxygen adsorbed on the surface of SnO2 nanospheres (**Figure 7**).

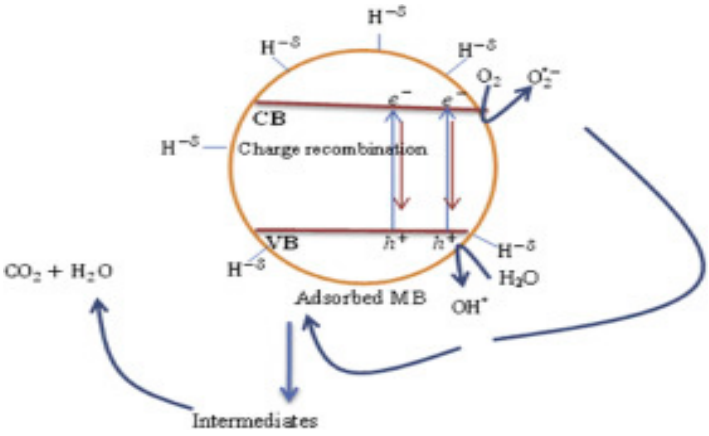

Figure 7: The photodegradation mechanism of MB/CB on SnO_2 nanospheres under UV-Visible irradiation.

The photoactivation of SnO_2 can be represented as follows:

$SnO_2 + h\nu \rightarrow SnO_2^* \rightarrow e^-CB + h^+VB \rightarrow$ recombination $\rightarrow$heat
$O2 + e^-CB \rightarrow O2^- + H2O \rightarrow OH^- + HO2^*$
$HO_2^* + HO2^* \rightarrow H2O2$
$h^+VB + OH^- \rightarrow HO^* + MB \rightarrow$ degradation products

From the suggested mechanism, one can notice that the OH radical produced on the surface of SnO2 takes part in photodecomposition. For example, in the case of CB, the -Cl is substituted by the OH species and transform into phenol. The phenol in turn undergoes hydroxylation to give rise to hydroquinone, which further oxidized to benzoquinone. Finally, the benzoquinone breaks down to CO_2 and H_2O [15]. There is no permanent adsorption of pollutant on the surface of SnO_2.

Regeneration of SnO_2 nanospheres was done to ensure whether the nanospheres can be re-used. The check the reusability, experiments were carried out on the spent SnO_2 nanospheres after washing it with distilled water for several times. The regenerated samples were dried in hot air oven at 100°C and re-run in an identical manner. Except a small change in photo efficiency, the results were comparable. Our results have shown that the photo efficiency was found to be around 90% even after using it for 5 cycles as shown in Figure 8 a & b. Since, the SnO_2 nanospheres are insoluble in water, separation of it was much easier from the reaction mixture.

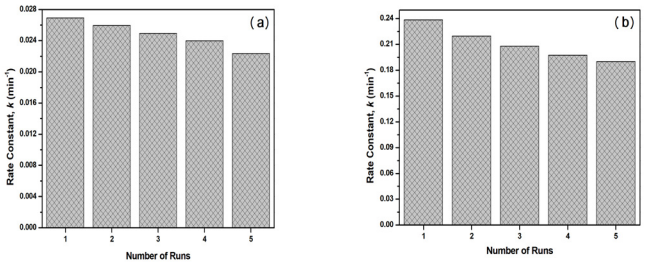

Figure 8: Photo efficiency of SnO_2 nanospheres on reusability for (a) methylene blue; and (b) chlorobenzene.

The slight decrease in photoactivity may be attributed to the blockage of pores inside SnO_2 nanospheres.

The slight decrease in photoactivity may be attributed to the blockage of pores inside SnO2 nanospheres.

Conclusion

Mesoporous tin oxide (SnO2) nanospheres were prepared by adding two types of surfactants. TEM images of SnO2 confirmed that the particles were spherical in shape with size ranges between 2 and 5 nm. At a surfactant solution concentration of 0.25 M, the BET surface was observed to be high (104 m^2g^{-1}) and this suggest the formation of lamellar structure of SnO_2 nanospheres. The nano samples prepared using only pure surfactant, had less surface area as compared to the one prepared from a mixture of cationic and anionic surfactants. This suggests that surfactant addition was very important aspect as it influences particle growth, coagulation, surface area, pore diameter and other factors. The photo study showed that when SnO_2 nanospheres were used as photocatalyst, the MB and CB were degraded up to 80% and 93 %, respectively. According to the pseudo 1st order kinetics, the reaction constant (k) for methylene blue was observed as 0.02693 and 0.2385 min^{-1} and for chlorobenzene, it was 0.02136 and 0.2023 min^{-1} under UV and Visible light, respectively.

Acknowledgement

Authors like to thank to Department of Science and Technology, India for their financial assistance.

References

1. Rauf MA, Ashraf SS (2009) Radiation induced degradation of dyes- an overview. Journal of Hazardous Materials 166: 6-16.
2. Sen L, Zhang Y, Yu B, Wang Z, Zhao H, et al. (2015) Solvent-free infiltration method to prepare mesoporous SnO2 templated by SiO2 nanoparticles for ethanol sensing. Sensors and Actuators B: Chemical 210: 700-705.
3. Guang Yin L, Wang H, Jin B, Yang Z, Qi W, et al. (2013) Synthesis and Electrochemical Properties of Mesoporous SnO2/C Composites as Anode Materials for Lithium Ion Batteries. International Journal of Electrochemical Science 8: 4797-4806.
4. Luyang Y, Hyodo T, Shimizu Y, Egashira M (2011) Preparation of mesoporous and/or macroporous SnO2-based powders and their gas-sensing properties as thick film sensors. Sensors 11: 1261-1276.
5. Liping L, Chen S, Xu L, Bai Y, Nie Z, et al. (2014) Template-free synthesis of uniform mesoporous SnO2 nanospheres for efficient phosphopeptide enrichment. Journal of Materials Chemistry B 2: 1121-1124.
6. Suraj TK, Mishr A, Jha SK, Rizwan Wahab R, Al-Khedhairy AA, et al. (2013) Microwave assisted hydrothermal synthesis of mesoporous SnO2 nanoparticles for ethanol sensing and degradation. Journal of Materials Science: Materials in Electronics 24: 2082-2090.
7. Li WC, Lu AH, Weidenthaler C, Schüth F (2004) Hard-templating pathway to create mesoporous magnesium oxide. Chem Materials 16: 5676-5681.
8. Li X, Xiao W, He G, Zheng W, Yu N, et al. (2012) Pore size and surface area control of MgO nanostructures using a surfactant-templated hydrothermal process: high adsorption capability to azo dyes. Colloids Surf A 408: 79-86.
9. Maerle A, Kasyanov I, Moskovskaya I, Romanovsky B (2016) Mesoporous, Synthesis, physico-chemical, and catalytic properties of MgO. Russian Journal of Physical Chemistry A 90: 1212–1216.
10. Wu Y, Bose S (2005) Nanocrystalline hydroxyapatite: micelle templated synthesis and characterization. Langmuir 21: 3232-3234.
11. Andreozzi P, Funari SS, Mesa CL, Mariani P, Ortore MG, et al. (2010) Multi-to unilamellar transitions in catanionic vesicles. Journal of Physical Chemistry B 114: 8056-8060.
12. Morsy J, Salwa MI (2014) Role of surfactants in nanotechnology and their applications. International Journal of Current Microbiology and Applied Sciences 3: 237-260.
13. Gnanam S, Rajendran V (2010) Anionic, cationic and nonionic surfactants-assisted hydrothermal synthesis of tin oxide nanoparticles and their photoluminescence property. Journal of Nanomaterials and Biostructures 5: 623-629.
14. Jeevanandam P, Klabunde K (2003) Redispersion and reactivity studies on surfactant coated magnesium oxide nanoparticles. Langmuir 19: 5491-5495.
15. Kibanova D, Trejo M, Destaillats H, Silva JC (2009) Synthesis of hectoriteTiO2 and kaolinite-TiO2 nanocomposites with photocatalytic activity for the degradation of model air pollutants. Applied Clay Science 42: 563-568.

Copyright: *©2020 Ashish Kumar, et al. This is an open-access article distributed under the terms of the Creative Commons Attribution License, which permits unrestricted use, distribution, and reproduction in any medium, provided the original author and source are credited.*